

A Fuzzy Logic Voltage Controller for Off-Grid Wind Turbine/Supercapacitor Renewable Energy Source

Ismail Hakki ALTAS¹ and Onur Ozdal MENGI²

¹Karadeniz Technical University Engineering Faculty Trabzon, Turkey
ihaltas@ktu.edu.tr

²Giresun University Engineering Faculty Giresun, Turkey
onurmengi@yahoo.com

Abstract

The amplitude and frequency of the voltage obtained from renewable energy sources change because the environmental conditions change continuously. This situation causes ripples, harmonics and faults on loads. Therefore, it is important to fix the voltage on the load busses. In wind energy systems, continuous change in wind speed results in varying load voltage. In order to discard this situation, there is a need for controlled power conditioning devices which will fix the voltage at desired levels. In this paper, a Fuzzy Logic Controller (FLC) which is designed to stabilize the voltage value of the load busses fed by Wind Turbine/Supercapacitor (WT/SC) hybrid energy system. The improvement obtained with the proposed method is depicted by comparing the results with those of PI controller. All the system is designed in MATLAB/Simulink environment.

1. Introduction

Lately, the studies on wind energy have increased rapidly all over the world. There may be various reasons of the interest in wind energy. However, the major reasons are the energy demand, environmental issues and the concerns about the reserves of the conventional energy sources such as oil and natural gas. Along with the other renewable energy sources, the wind energy gets high attention, probably the most one. Hence, wind turbines and different energy storage systems have become important sources and devices [1,2].

It is obvious that wind energy is a widely used renewable energy source. Since the electricity is produced from the variable speed of the wind, the magnitude of the generated voltage and its frequency are also variable. However, the voltage at load busses must have constant magnitude and frequency since the commercially available appliances and loads are manufactured to be operated at standard voltage and frequency values. Therefore the operating conditions and power quality issues have to be considered in wind energy systems. That is where the power conditioning devices become important. In order to stabilize and control the voltage, different schemes have been studied and introduced in literature. Some researchers suggest the scheme with an AC/DC then DC/AC link [3] while some suggest just AC/AC converters with magnitude and frequency control ability [4]. Besides using DC link and/or converters supporting active and passive filtering are also employed for power conditioning and voltage-frequency stabilization [5]. Controlling the power electronics converters and the filters is also important as much as designing the

converters and filters. Therefore studies on power electronics converter used in wind energy systems are always accompanied by controllers. It is possible to find many works on designing controllers for the converters in wind energy systems [2].

A DC link used in this study as the main interface between the wind generator and the AC load bus as shown in Figure 1. The voltage from the wind turbine is converted to DC using a rectifier. Then a DC link filter is used to stabilize the voltage magnitude before it is converted to AC by a controlled IGBT inverter. After the inverter, an AC filter is employed to smooth the current ripples while maintain a constant voltage magnitude. During this process, the amplitude of the voltage is set by the rectifier and DC filter and frequency is controlled by the inverter. Therefore the magnitude and the frequency of the voltage at load bus are kept at desired standard values. The proposed scheme has two additional parts, which are the supercapacitor and the controller. The supercapacitor acts to prevent the loads from being powerless as a result of sudden change in wind speed. A 50 kW load is used as a load in the system.

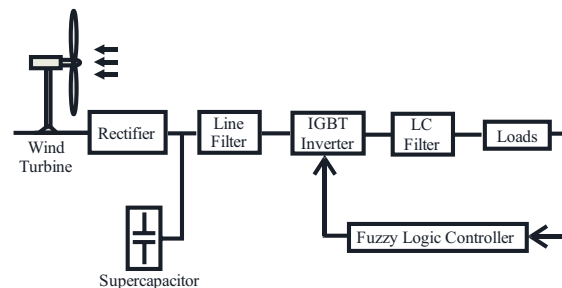


Fig. 1. Wind/SC renewable energy source

The system responses are obtained and analyzed for two operating cases. The case when there are rapid changes in wind speed and the case when there are sudden load changes and excursions.

2. The Wind Energy Conversion Scheme

The proposed wind energy conversion scheme (WECS) is shown in Figure 1. As it is depicted, the scheme consists of a wind turbine including a coupled induction generator, a rectifier, a supercapacitor, an inverter, loads, FLC, and filters.

2.1. Wind Turbine

Wind turbines convert wind speed to rotational mechanical torque, which is used by electrical generators to produce electrical energy. Usually synchronous, asynchronous or direct current generators are used in wind turbines. The asynchronous generator used in this simulation.

Wind turbine model is developed taking steady state power characteristics into consideration. The mechanical power produced by the wind turbine can be given as

$$P_m = \frac{1}{2} C_p(\lambda, \beta) \rho A v^3 \quad (1)$$

Where, P_m represents mechanical output power of the turbine (W), C_p is the performance coefficient, λ is pitch angle (degree), β is peak speed rate, ρ is the air density (kg/m^3), A is rotor sweep area (m^2) and v is the wind speed (m/s). $C_p(\lambda, \beta)$ is calculated.

As follows.

$$C_p(\lambda, \beta) = C_1 \left(\frac{C_2}{\lambda_1} - C_3 \beta - C_4 \right) e^{\frac{C_5}{\lambda_1}} + C_6 \lambda \quad (2)$$

Where;

$$\frac{1}{\lambda_1} = \frac{1}{\lambda + 0.08\beta} - \frac{0.035}{\beta^3 + 1} \quad (3)$$

The values used here are $C_1=0.5176$, $C_2=116$, $C_3=0.4$, $C_4=5$, $C_5=21$ and $C_6=0.0068$. β value is taken as 0 [6,7].

2.2. Supercapacitor Equivalent Circuit

The devices called as ultracapacitors or supercapacitors are used for energy storage and filtering processes. They are used in high power discharging applications. Owing to their high energy density, they have the capacity to send hundreds of amperes current. Their usage increases because they can provide short time sudden power need. They achieve this without any chemical process. Being unmaintained and durable are other characteristics of these machines [8]. The internal structure of the supercapacitor can be seen in Figure 2.

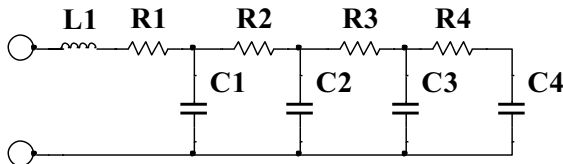


Fig. 2. The equivalent circuit model of the supercapacitor

The equation representing the charging case of the supercapacitor is:

$$\text{SOC} = 1 - [V_{\text{rated}} - V / (V_{\text{rated}} / 2)] \quad (4)$$

Where V is the terminal voltage of supercapacitor [9].

2.3. Fuzzy Logic Controller

After the invention of fuzzy logic by L.A. Zadeh in 1965 [10] and its application to control systems by Mamdani in mid 1970s [11], so many researches and applications done related to fuzzy logic controller. Although some reasoning algorithms, such as Sugeno and TSK algorithms [12], have been developed, Mamdani reasoning algorithm is used widely. Actually the fuzzy logic control (FLC) algorithms in all fuzzy reasoning methods have the similar structure consisting of a fuzzifier, a rule base a fuzzy reasoning and a defuzzifier as shown in Figure 3.

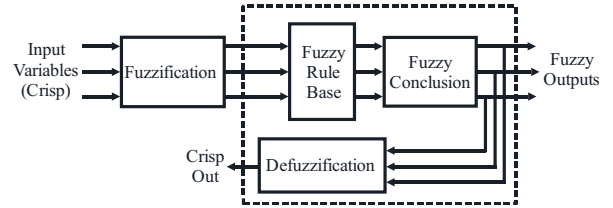


Fig. 3. Basic configuration of a FLC.

If the inputs are crisp, as they are in this study, they are converted to fuzzy membership values by the fuzzifier first. Then, the rule base evaluates these fuzzy membership values so that a fuzzy output can be yielded after running a fuzzy reasoning process. If a crisp output is required as in Mamdani reasoning algorithm, the defuzzifier stage is employed to convert the fuzzy output to a crisp output.

The main elements of FLC are membership functions. Triangle membership functions seen in Figure 4 are used to define fuzzy membership functions at the input and output spaces of the FLC. The fuzzy membership value of the variable x in fuzzy subset A represented by a triangle membership function is calculated by using equation (5).

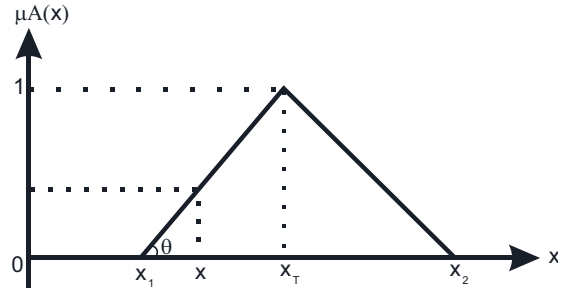


Fig. 4. Triangle membership function

$$\mu_A(x) = \max \left(\min \left(\frac{x - x_1}{x_T - x_1}, \frac{x_2 - x}{x_2 - x_T} \right), 0 \right) \quad (5)$$

The FLC algorithm defined above has been used in many applications. The one used here is a modification of the algorithm studied in [13]. This algorithm is nothing but a Matlab/Simulink model of Mamdani algorithm. It is modified for this study to suit the problem studied here.

The error e and its change de in every sampling are two inputs the fuzzification and rule base block. Parameters of triangular fuzzy subsets shown in Figures 5 and 6 are also the

inputs to fuzzifier and rule base block. Since there are five fuzzy subsets for e and five other fuzzy subsets for de, a 25 rule based is processed inside the block using the verbal implication as

If x is A and y is B then z is C.

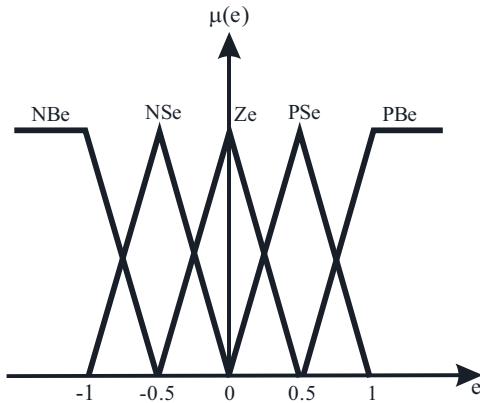


Fig. 5. Error membership functions

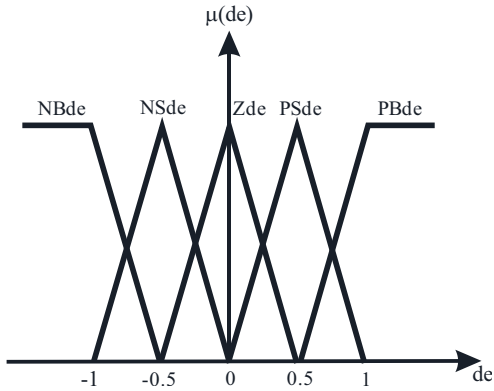


Fig. 6. Variation of error membership functions

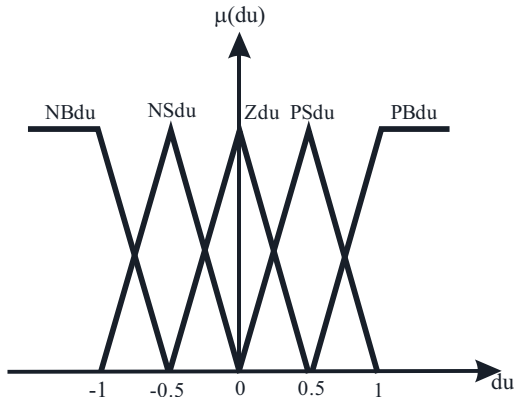


Fig. 7. Output space

Where x is e, y is de, z is du and A, B, and C are the fuzzy subsets in the universes of e (error), de (error change) and du (output), respectively. Here, NB is negative big, NS is negative

small, Z is zero, PS is positive small and PB is positive big. The membership values generated by the rule base for the output space are used along with the parameters of triangular fuzzy subsets given in Figure 7 of the output space in the block called Defuzzification 1, which is nothing but the process of the numerator of defuzzification method called center of area. The block Defuzzification 2 represents the denominator of the center of area method. The final output of the FLC is the division of Defuzzification 1 by Defuzzification 2, which is the result of defuzzification formula called the center of area method [13]. The main Simulink block diagram of the FLC used in this study is given Figure 8.

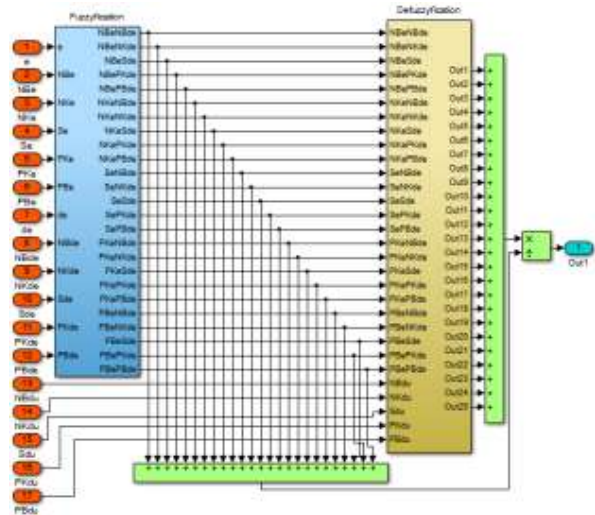


Fig. 8. Simulink model of defuzzification process

3. System Simulation

The simulated system can be seen in Figure 9. Here, the system consists of a 60 kW wind turbine, rectifier, line filter, inverter, load filter, 50 kW resistive load and controller. The simulation is done to keep the line-to-line voltage at 380 V and 50 Hz during the changes in wind speed.

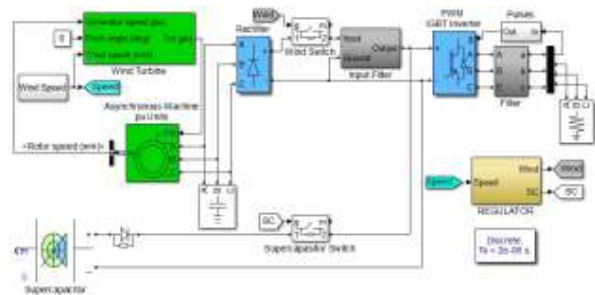


Fig. 9. Simulation system

When the wind speed is sufficient, the whole system is supplied by the wind turbine; otherwise, the supercapacitor is turned on to supply the system. The DC voltage produced by the wind/supercapacitor system is converted to AC voltage using a 3-phase inverter in order to supply power to the 3-phase

load. The voltage output of the inverter is controlled to keep the voltage at 380 V, line to line, at a fixed frequency of 50 Hz. The 3-phase voltages are converted to d-q axis layouts as direct-axis voltage V_d and quadrature voltage V_q , to be used by the PI controller and the FLC. The output of the controller is then used to generate a pulse-width modulated signal, which is used to control the output voltage of the inverter. The frequency of the inverter is controlled and kept constant at 50 Hz through a phase-locked loop process.

There is a filter (LC) parallel to the loads so as to straighten the wave shape of the voltage on the load in the system. The wave shape of the load voltage is tried to be straightened. During this time, total harmonic distortion is measured as well.

The regulator that is used is a system which does measurements and switching in order to activate the supercapacitor when the wind speed falls under 5 m/s.

The changes in the environment affect the working of system. Therefore, it is aimed to create different environmental conditions by changing the wind speed level. The wind speed is changed as seen in Figure 10.

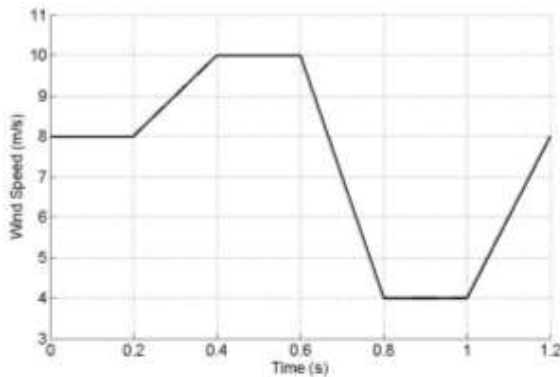


Fig. 10. Wind speed

4. Discussion and Result Analysis

The results obtained by using PI controller are given in Figures 11-14. In Figure 11, it is seen that PI controller does not set at 380 V value. The supercapacitor is active since there is not enough wind speed at $t=0.8-1$ s period; therefore, the voltage on the load sets at 380V value in this period. The Total Harmonic Distortion (THD) change during the simulation with PI controller goes up to 0.2 as shown in Figure 12. Distorted wave shape across the load terminals is given in Figure 13. The distortion in the voltage wave shape is because of the changes in the wind speed. Even if there is supercapacitor in the circuit the harmonics are not being eliminated completely. Figure 14 shows the error which is below 0.4.

The results obtained by using FLC are given in Figures 15 to 18. The voltage on the load bus is 380 V with some ripples as shown in Figure 15. Supercapacitor is active during $t=0.8-1$ s period for this case as in the case with the PI controller. The THD change for the case with FLC is below 0.2 as depicted in Figure 16. In Figure 17, the wave shape of the voltage on the load is shown. This wave shape is very close to sine wave. In Figure 18, the time response of the error is given. The error value is below 0.4 for this case.

5. Conclusions

When the graphs between Figure 11 and 18 are analyzed, in simulations conducted with both PI and FLC controller, it is seen that the voltage on the load is pretty distorted in PI controller. When FLC is used, it is seen that this distortion decreases. The difference is very obvious in Figures 12 and 16. When THD values are analyzed, it is seen that there is not a significant difference. Similarly, error values vary more or less the same. FLC's maximum exceeding is a high value as 450 V.

However, since the voltage on the load is very different from 380 V with PI controller, it is not preferred to be used. There is very little ripple with FLC and it sets to 380 V value. Obviously, FLC puts forward more qualified results than PI controller.

6. References

- [1] S.M. Muyeen, "Wind Energy Conversion Systems", Springer, London, UK, 2012.
- [2] A. Lara, N. Jankins, J. Ekanakaye, P. Cartwright and M. Hughes "Wind Energy Generation Modelling and Control", Wiley, UK, 2009.
- [3] J. F. Manwell, J. G. Mcgovan and A. L. Rogers, "Wind Energy Explained Theory, Design and Application 2e", Wiley, London, UK, 2009.
- [4] C. L. Kana, M. Thamodharan and A. Wolf, "System Management of a Wind-Energy Converter", *IEEE Transactions on Power Electronics*, Vol.16, Issue.3, 2001, pp.375-381.
- [5] C. Wnag and M. H. Nehrir, "Power Management of a Stand-Alone Wind/Photovoltaic/Fuel Cell Energy System", *IEEE Transactions on Energy Conversion*, Vol.23, Issue.3, 2008, pp.3957-967.
- [6] O. O. Mengi and I. H. Altas, "Wind/Battery Renewable Energy Production System", *Turkish Journal of Electrical Engineering and Computer Sciences (TJEECS)*, TUBITAK, Vol:20, Issue:2, Turkey, 2012, pp:187-206.
- [7] S. Voller, A. R. Awaad and J. F. Verstege, "Wind Farms with Energy Storages Integrated at The Control Power Market", *CIGRE/IEEE PES Joint Symp.*, 2009, pp.1-13.
- [8] B. Kocaman, "Akıllı Sebekeler ve Mikro Sebekelerde Enerji Depolama Teknolojileri", *Akıllı Sebekeler ve Türkiye Elektrik Sebekesinin Geleceği Semp.*, Ankara, 26-27 2013.
- [9] H. Babazadeh, W. Gao, J. Lin ve L. Cheng, "Sizing of Battery and Supercapacitor in a Hybrid Energy Storage System for Wind Turbines", *Transmission and Distribution Conference and Exposition*, 7-10 May 2012, p:1-7.
- [10] L.A. Zadeh, "Fuzzy Sets", *Information and Control*, Vol:8, pp.338-353, 1965.
- [11] T.J. Ross, "Fuzzy Logic with Engineering Applications", John Wiley and Sons, London, England, 2004.
- [12] N. Baykan ve T. Beyan, "Bulanik Mantik Uzman Sistemler ve Denetleyiciler", *Bicaklar Kitapevi*, Istanbul, 2004.
- [13] I. H. Altas and A. M. Sharaf, "A Generalized Direct Approach for Designing Fuzzy Logic Controllers in Matlab/Simulink GUI Environment", *International Journal of Information Technology and Intelligent Computing*, Int. J. IT&IC No.4, Vol:1, 2007.

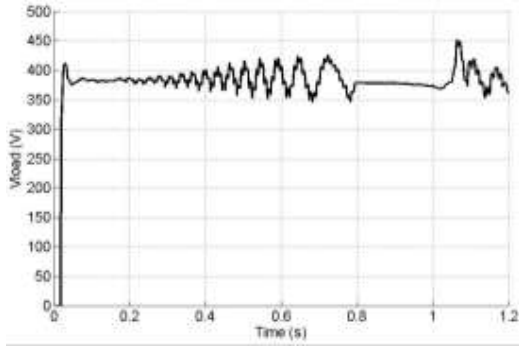


Fig. 11. The result of PI controller, V_{load} variation

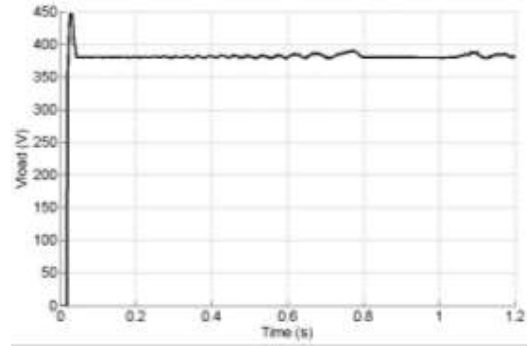


Fig. 15. The result of FLC controller, V_{load} variation

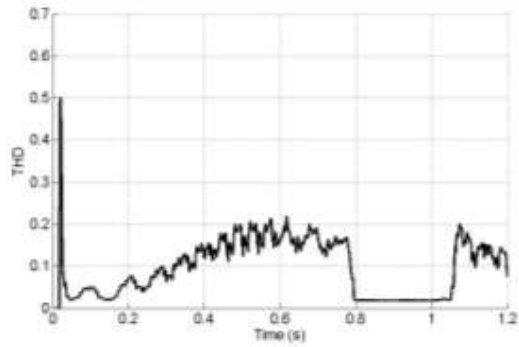


Fig. 12. PI controller THD exchange

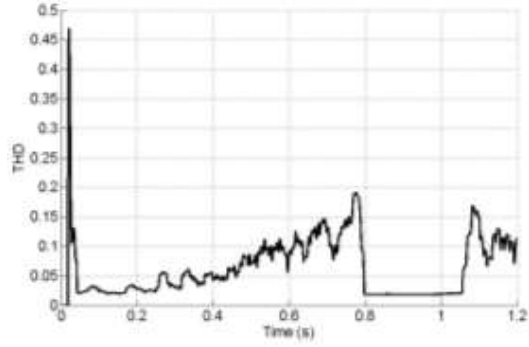


Fig. 16. FLC THD exchange

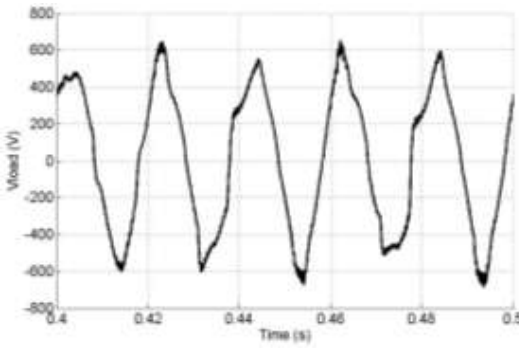


Fig. 13. V_{load} variation for the PI controller

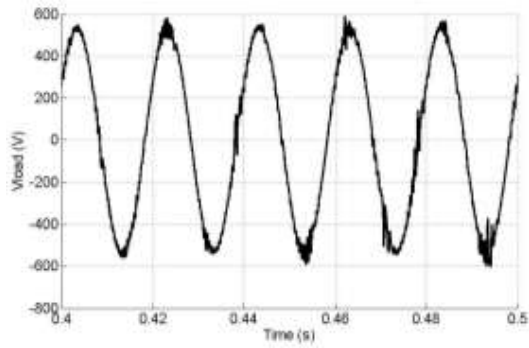


Fig. 17. V_{load} variation for the FLC

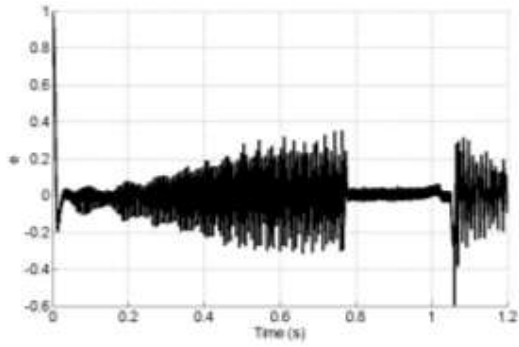


Fig. 14. PI controller error change

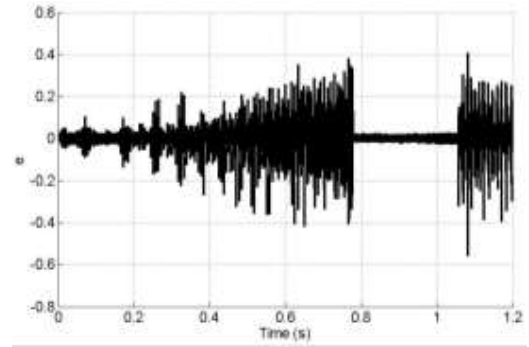


Fig. 18. FLC error change